INFLUENCE ON UNCERTAINTY OF EARTHQUAKE RESPONSE ANALYSIS RESULTS BY INITIAL PARTICLE ARRANGEMENTS AND COHESION PARAMETERS IN EXTENDED DISTINCT ELEMENT METHOD

- PARTICLES 2019

TAIKI. YOSHIDA[1], HITOSHI. TOCHIGI[2]

[1] Central Research Institute of Electric Power Industry (CRIEPI)
Earthquake Engineering Sector Civil Engineering Research Laboratory
1646 Abiko, Abiko-sh, Chiba 270-1194 JAPAN
taiki@criepi.denken.or.jp and https://criepi.denken.or.jp/

[2] Central Research Institute of Electric Power Industry (CRIEPI)
Earthquake Engineering Sector Civil Engineering Research Laboratory
1646 Abiko, Abiko-sh, Chiba 270-1194 JAPAN
tochigi@criepi.denken.or.jp and https://criepi.denken.or.jp/

Key words: EDEM, Impact Force, Uncertainty, Cohesion.

Abstract Following the occurrence of extremely large earthquakes, such as the Great East Japan Earthquake, the level of design for earthquake ground motion in nuclear power plants has been enhanced. Additionally, the quantitative evaluation of the seismic performance of critical facilities, such as nuclear power plants, and earthquake-induced failure of surrounding slopes are becoming increasingly important as deterministic approaches in regulation. However, evaluation of other aspects besides the design for earthquake ground motion in probabilistic risk assessment (PRA) needs to be conducted voluntarily by the corporation.

For the earthquake response analysis, including the seamless transition of the slope from continuum to dis-continuum, the extended distinct element method (EDEM) is an effective approach; however, EDEM is characterised by initial particle arrangement uncertainty. Therefore, we investigated the uncertainty in the EDEM results with respect to failure timing and region. Although essential in the evaluation of impact force in the PRA framework, there are few researches regarding the uncertainty of impact force on the wall of the reactor building after slope failure caused by numerous initial particle arrangements. Furthermore, reducing the computational time is crucial in PRA. Hence, the parameters that do not have an influence on the EDEM results can be omitted, resulting in their dispersion and a reduction in the computational time.

This research aims to investigate the impact force uncertainty caused by initial particle arrangements and the influence of cohesion uncertainty. For the former, we conducted 50 numerical simulations for the uncertainty of EDEM results caused by the initial particle arrangements. For the latter, we conducted 50 numerical simulations with two uncertainty factors, namely, cohesion and initial particle arrangement.

The simulation results revealed that the largest and second largest loads on the wall occurred in two cases, namely, when there were single particles impacting the wall and when there were group particles impacting the wall. Additionally, the uncertainty caused by cohesion was less than that caused by the initial particle arrangement when the coefficient of variation was 0.1. Thus, the cohesion uncertainty can be ignored if it is somewhat small.

1 INTRODUCTION

Following the occurrence of extremely large earthquakes, such as the Great East Japan Earthquake, the level of design for earthquake ground motion in nuclear power plants has been enhanced. Additionally, the quantitative evaluation for the seismic performance of critical facilities, such as nuclear power plants, and earthquake-induced failure of surrounding slopes are becoming increasingly important as deterministic approaches in regulation. However, the evaluation of other aspects besides the design for earthquake ground motion in probabilistic risk assessment (PRA) needs to be voluntarily conducted by the corporation.

The seismic stability of the surrounding slopes on the basis of ground displacement is often determined using the finite element method (FEM). For example, the Central Research Institute of Electric Power Industry (CRIEPI) recommends a time history nonlinear analysis for evaluating the stability of slopes, including post-earthquake residual displacement, and predicting a failure range when large deformations and displacements occur [1].

For the evaluation of rock mass displacement, once the failure of the slope model has been confirmed by FEM, the distinct element method (DEM) is often used. This is a discontinuous analysis method [2], which can easily evaluate large deformations or failures in comparison with FEM.

Moreover, the earthquake response analysis of the slope, including its seamless transition from continuum to dis-continuum can be better than the method, which is divided into two steps which are the stability evaluation by FEM and the one of rock mass displacement by DEM.

The extended distinct element method (EDEM) may be effective for developing such a seamless analytical approach [3]. In the EDEM, a pore spring exists among the soil pores for cohesion between particles. By setting the tensile strength and shear strength between particles and turning off the pore spring when the pore force exceeds the tensile and shear strengths, the progressive failure of the slopes can be modelled.

EDEM is characterised by the initial particle arrangement uncertainty. Therefore, we investigated the uncertainty in EDEM results with respect to failure timing and region [4,5]. The probability distribution of the inclination angle was similar to the normal distribution when a slope fails and most of the slip lines defined in the analysis were near the slip lines in the experiment. Yoshida et al. investigated the influence of initial particle arrangements using the moving particle simulation (MPS) [6].
Although essential in the evaluation of impact force in the PRA framework, there are few studies on the uncertainty of impact force on the wall of a reactor building after slope failure caused by several initial particle arrangements. Furthermore, reducing the computational time is critical in PRA. Thus, the parameters that do not have any influence on the EDEM results can be omitted, resulting in their dispersion and a reduction in the computational time.

This research has two purposes, which are to investigate the impact force uncertainty caused by initial particle arrangements and the influence of cohesion uncertainty. For the former, we conducted 50 numerical simulations for the uncertainty of EDEM results caused by initial particle arrangements. Additionally, for the latter, we conducted 50 numerical simulations with two uncertainty factors, namely, cohesion and initial particle arrangement.

2   SHAKING TABLE MODEL TEST

The geo-materials used to construct the slope model comprised stainless particles, iron sand, and water, which were mixed in the ratio of 40:30:1. The physical parameters were obtained from laboratory results of a plane strain compression test, cyclic tri-axial test, and uniaxial tension test, as presented in Table 1 (σ indicates the confining pressure).

Table 1: Physical properties of geo-materials

Physical property	Value
Wet unit weight [kg/m^3]	4.20×10^3
Poisson ratio [-]	9.00×10^{-2}
Static elastic modulus [MPa]	$1.36 \cdot \sigma^{1.03}$
Initial shear elastic modulus [MPa]	$34.44 \cdot \sigma^{0.32}$
Tensile strength [kPa]	0.5
Peak shear strength [kPa]	$7.0 + \sigma \cdot \tan 40.9°$
Residual shear strength [kPa]	$2.05 \cdot \sigma^{0.69}$

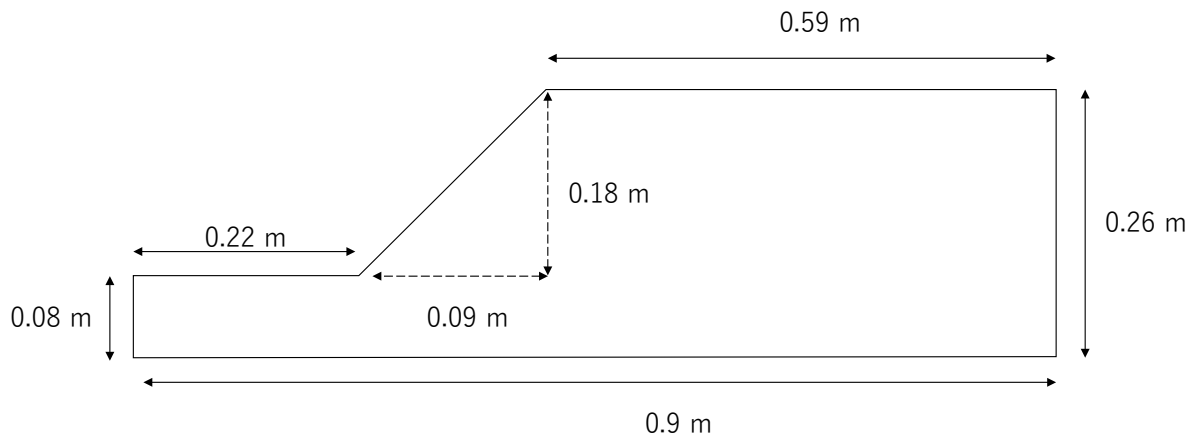The scale of the slope model, with a slope gradient of 1:0.5, is illustrated in Figure 1.

Figure 1: Scale of slope model

The model was shaken in 16 stages at input accelerations. The input acceleration was a sinusoidal waveform, with the main section consisting of 20 waves at a frequency of 20 Hz. The horizontal acceleration waveform measured at the bottom of the soil bin in this test is illustrated as an example in Figure 2.
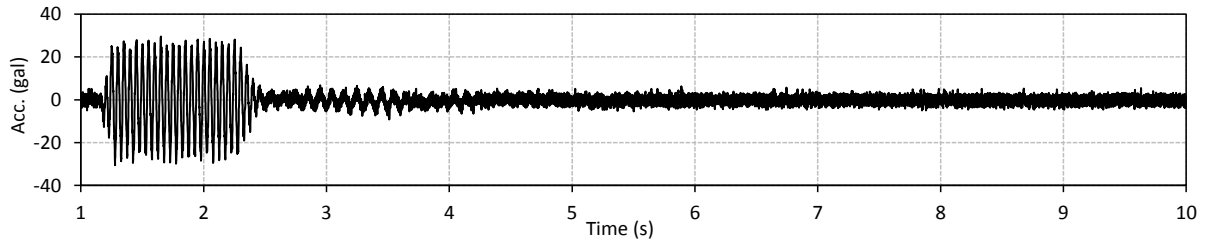
Figure 2: Horizontal acceleration measured at the bottom of the soil bin during the third stage of the shaking table model test

3 DISTINCT ELEMENT METHOD (DEM) FOR SOFT ROCK

For the numerical simulation, we used Itasca PFC3D code and constrained particles that were moving out from the plane direction to model the granular materials as a 2D analysis. When calculating the force between the particles, a spring coefficient was used to obtain the contact force, a viscous damping coefficient was used to determine the energy attenuation, a divider was used to ignore the tensile force, and a slider was used to determine the dynamic frictional force. The initial particle cohesion was modelled as a parallel bond, and the motion of each particle is expressed as follows:

$$\frac{d\boldsymbol{P}}{dt} = \sum \boldsymbol{F} \tag{1}$$

$$\frac{d\boldsymbol{L}}{dt} = \sum \boldsymbol{N} \tag{2}$$

Here, $\boldsymbol{P}$ represents the linear momentum, $\boldsymbol{F}$ represents the force acting on the soil element, $\boldsymbol{L}$ is the angular momentum, and $\boldsymbol{N}$ is the torque acting on the soil element.

To classify the material properties depending on confining pressure, we divided the slope model vertically into three layers, as depicted in Figure 4, where the red area represents 1.78 kPa, the blue area represents 5.35 kPa, and the green area represents 8.92 kPa in terms of confining pressure.
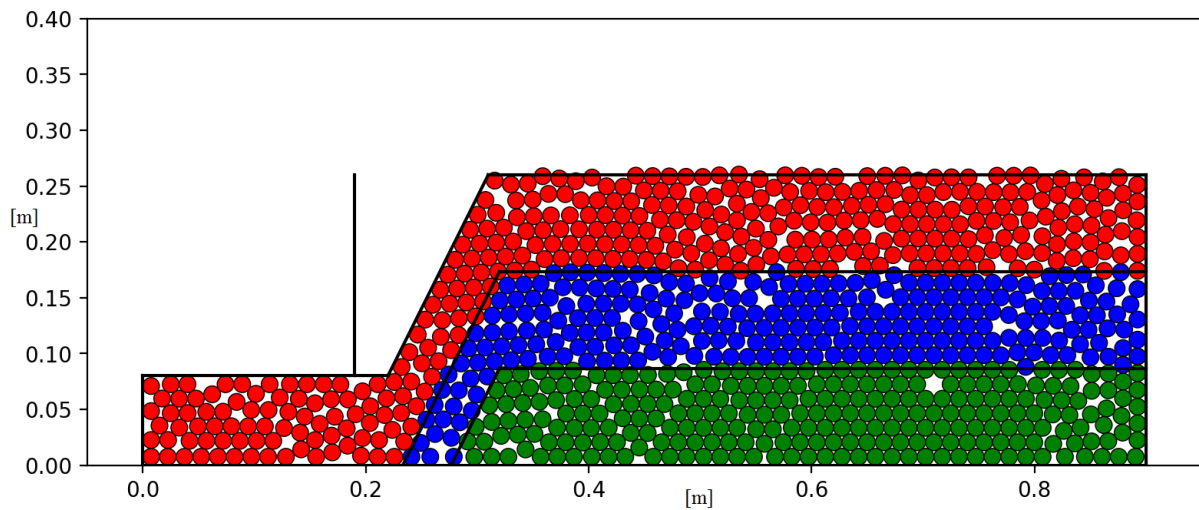
Figure 3: Example of analytical model of slope

For the boundary condition, the front and back of the slope were modelled as a rigid wall and the particles at the bottom of the soil bin, indicated in purple in Figure 3, were fixed.

Fifty models with varying initial particle arrangements were prepared. Each model was composed of particle whose diameter were 15 mm.

The DEM parameters for the contact force are listed in Table 2. The spring coefficient, pore spring coefficient, and shear strength were determined using the plane strain compression test, whereas the dynamic friction coefficients were determined using the cyclic tri-axial test. The tensile strength was obtained by the uniaxial tension test.

Table 2: DEM parameters for contact force

Layer number	First	Second	Third
Wet unit weight [kg/m^3]		4.20×10^3	
Normal spring coefficient [N/m]	4.25×10^7	5.51×10^7	6.51×10^7
Tangential spring coefficient [N/m]	1.92×10^7	2.48×10^7	2.93×10^7
Normal pore spring coefficient [N/m]	1.28×10^5	1.65×10^7	1.95×10^7
Tangential pore spring coefficient [N/m]	5.76×10^4	7.44×10^4	8.79×10^4
Normal damping ratio [%]		3	
Tangential damping ratio [%]		3	
Inter-particle friction angle [°]		34	

Inertial force was added to the centre of the particles using horizontal acceleration waveforms measured at the bottom of the soil bin in the shaking table model test. The shaking started only from the third stage in the numerical simulation because there was white noise excitation and a low response from the slope in the first two stages.

4 RESULTS AND DISCUSSION

4.1 Impact force

The impact force P can be calculated based on the elastic contact theory in EDEM analysis as follows:

$$P = \kappa \delta^n \tag{3}$$

$$\kappa = \frac{4}{3} E_0 \sqrt{R_0} \tag{4}$$

$$E_0 = \frac{1}{\frac{1-\nu_1^2}{E_1} + \frac{1-\nu_2^2}{E_2}} \tag{5}$$

$$R_0 = R \tag{6}$$

Here, P represents the impact force, κ represents the force acting on the soil element, δ is the amount of overlap, n is 1.5, E_0 is defined in equation (5), ν_1 is the Poisson's ratio of the wall, E_1 is the elastic modulus of the wall, ν_2 is the Poisson's ratio of the rock mass, E_2 is the elastic modulus of the rock mass, R_0 is defined in equation (6), and R is the particle radius depicted in Figure 4.
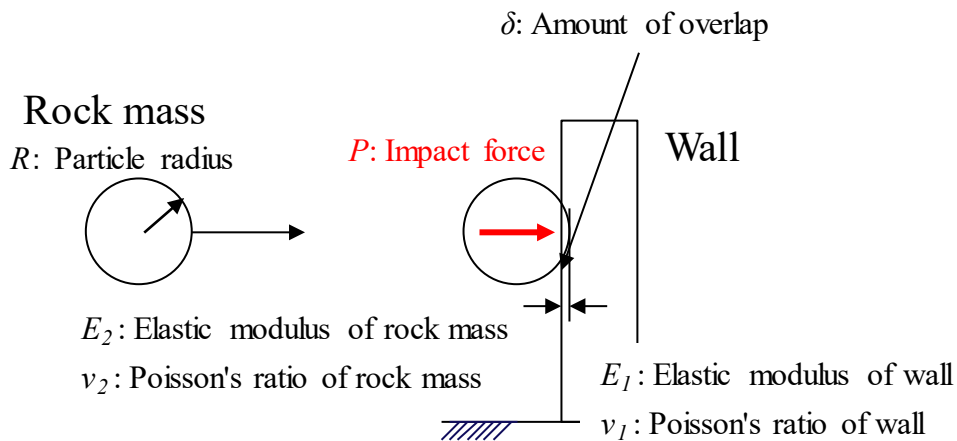

Figure 4: Parameters for impact force

The virtual rigid wall is located 3 cm away from the foot of the slope, as illustrated in Figure 3. Fifty numerical simulations were conducted with varying initial particle arrangements. Figure 5 illustrates the histogram of the maximum load on the wall.
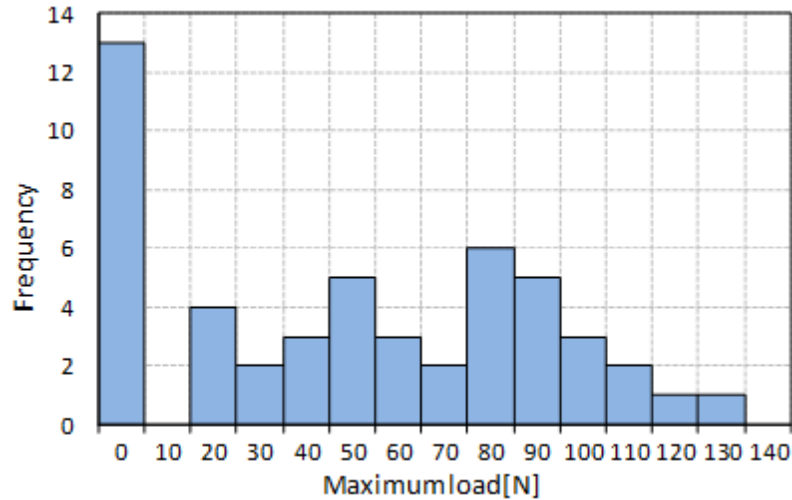

Figure 5: Histogram of maximum load on the wall

It can be observed from Figure 5 that the largest load is approximately 125 N in case 44 and the second largest load is approximately 117 N in case 22. It is important to clarify how features there are when the impact force is so large from these analytical results.

Figure 6 depicts the timing when the maximum load on the wall occurs in case 44, in which a single particle impacts the wall.
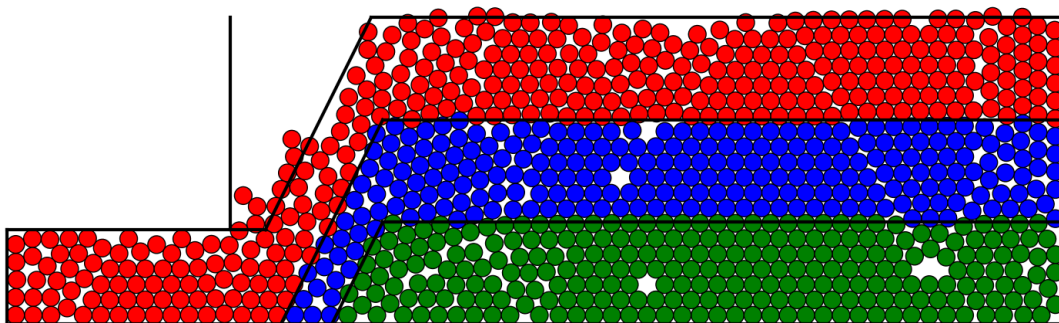

Figure 6: Timing of maximum load on the wall in case 44

On the other hand, Figure 7 depicts the timing when the maximum load on the wall occurs in case 22, in which a particle group impacts the wall.
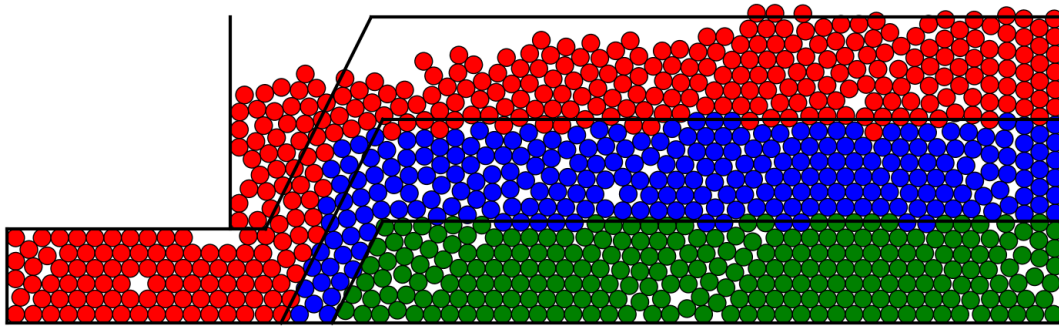

Figure 7: Timing of maximum load on the wall in case 22

According to the theoretical consideration, the impact force depends on the kinematic energy of the rock masses, as expressed in equation (5).

$$E = \frac{1}{2}MV^2$$
(5)

Here, **M** represents the mass of the rock and **V** represents the velocity of the rock.

In cases when the kinematic energy is high, there are two possibilities: the mass M can be extremely large or the velocity V is extremely high. Case 44 is interpreted as the former, and case 22 is interpreted as the latter.

4.2 Influence of initial particle arrangement on uncertainty

The frequency line graph of the numerical simulation results are depicted in Figure 8. In this analysis, failure timing is defined as the time when the average movement of particles near the top of the slope exceeds the threshold set for particle displacement.
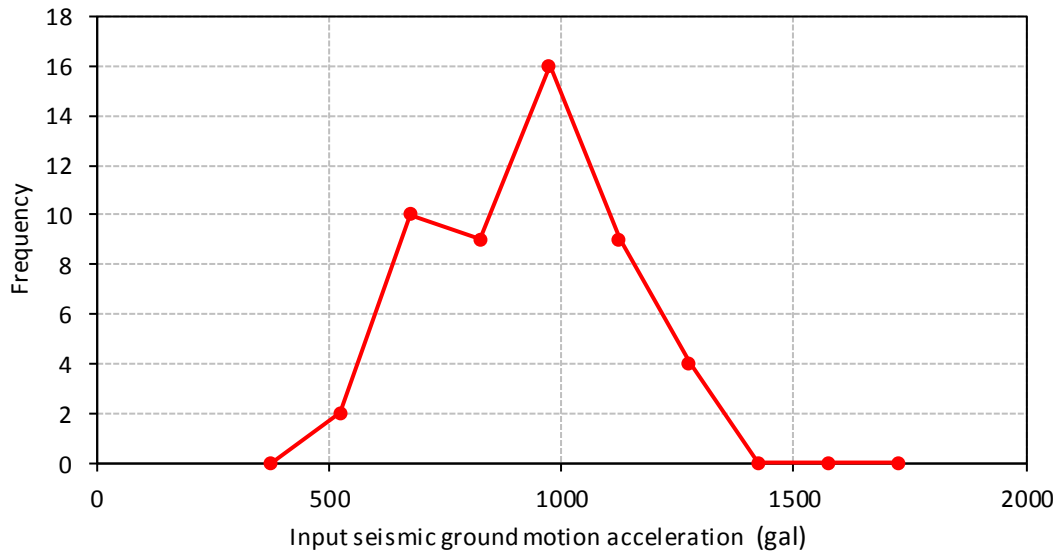
Figure 8: Frequency line graph of numerical simulation result

Based on the $\chi-$square test, the theoretical probability distribution is determined as a normal distribution. The average value of input seismic ground motion acceleration is approximately 902 gal and the coefficient of variation is 0.22.

4.3 Influence of cohesion and initial particle arrangement on uncertainty

Fifty numerical simulations were conducted with both cohesion parameters and initial particle arrangements. The purpose was to investigate the influence of the cohesion parameters on the uncertainty by comparing the results of only the initial particle arrangements with those of the cohesion parameters and initial particle arrangements.
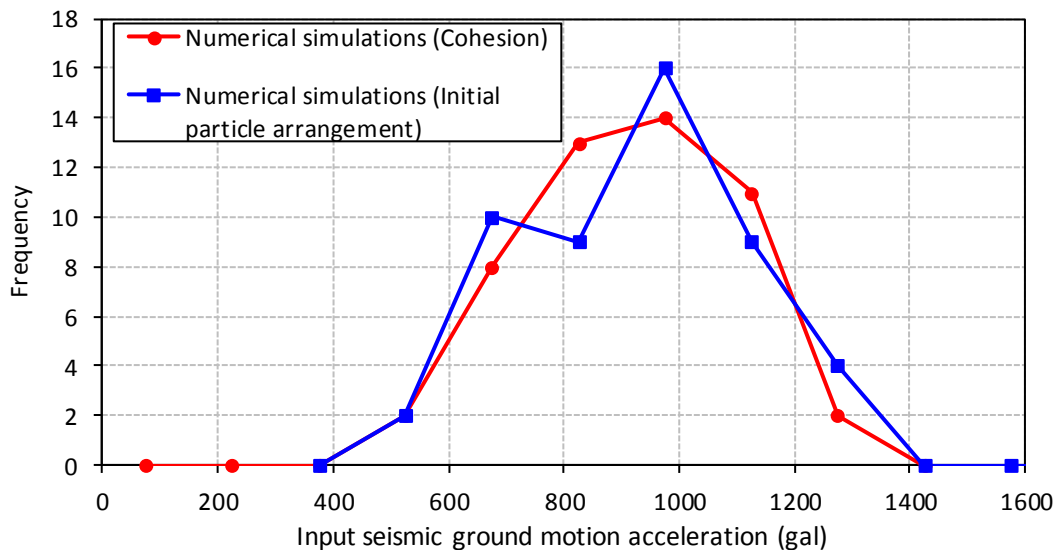

Figure 9: Frequency line graphs of two numerical simulation results from 50 cohesion parameters, whose coefficient of variation is 0.1, and initial particle arrangements
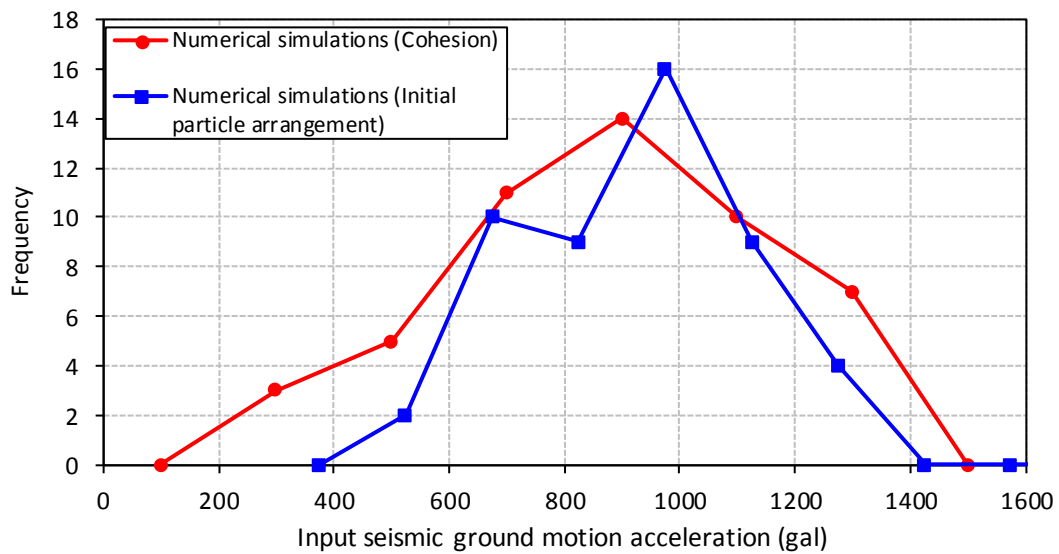
Figure 10: Frequency line graphs of two numerical simulation results from 50 cohesion parameters, whose coefficient of variation of 1.0, and initial particle arrangements

Figure 9 illustrates the frequency line graphs of the numerical simulation results with a coefficient of variation of 0.1. The average value of the input seismic ground motion acceleration is approximately 899 gal and the coefficient of variation from numerical simulations is 0.20.

On the other hand, Figure 10 depicts the frequency graph of the numerical simulation results with a coefficient of variation of 1.0. The average value of the input seismic ground motion acceleration is approximately 858 gal and the coefficient of variation from numerical simulations is 0.33.

In comparison with the results in Figure 9, the coefficient of variation is larger in Figure 10. It is also clarified that the coefficient of variation from the numerical simulations of the cohesion parameters and initial particle arrangements in Figure 9 is less than that of only the initial particle arrangements in Figure 8.

Based on these results, it can be concluded that the uncertainty of cohesion can be ignored if the coefficient of variation is somewhat small.

12 CONCLUSIONS

This research clarified two cases when the impact force is large. It is concluded that there are two possibilities: the mass M can be extremely large or the velocity V is extremely high. Additionally, the cohesion uncertainty was investigated. The results confirm that the influence of cohesion uncertainty can be ignored when its coefficient of variation is somewhat small.

In the future, we aim to clarify the range of the coefficient of variation, in which the influence of cohesion uncertainty can be ignored, and conduct the same investigation using other parameters.

REFERENCES

[1] Ishimaru, M., Okada, T., Nakamura, H., Kawai, T., Kazama, M. "*Modelling of strength and deformation characteristics after shear failure of soft rock and application to evaluation of seismic stability of slopes against sliding*," J. Jpn. Soc. Civil Eng. Ser. C, 73(1), pp. 23-38, (2017). (in Japanese)

[2] Tochigi, H., Nomura, Y., Ozawa, K. "*DEM analysis of falling rocks' reaching distance providing that surrounding slope in nuclear power plant facility failures*," (*Proc. Annu. Conf JSCE*), (2018). (in Japanese).

[3] Hakuno, M. "*Simulation of rupture-tracing rupture by an extended distinct element method*," Tokyo: Morikita Publishing Co., Ltd. (1997).

[4] Yoshida, T., Tochigi, H. "*Numerical Simulation on Inclining Model Experiment by Extended Distinct Element Method*," *Proceedings of the 52nd Japan National Conference on Geotechnical Engineering*, 0861, pp. 1719-1720, (2017). (in Japanese)

[5] Yoshida, T., Nakajima, M., Tochigi, H. "*Studying parameters for changing the initial particle arrangements of distinct element analysis in earthquake response based on slope analysis*," *Proceedings of 14th International Conference on Probabilistic Safety Assessment and Management (PSAM14)*, (2018).

[6] Yoshida, I. "*Basic study on failure analysis with using MPS method*," J. Jpn. Soc. Civil Eng. Ser. C, 73(1), pp. 93-104, (2011). (in Japanese)